Method for the rotational alignment of polarization-maintaining optical fibers and waveguides

Timo T. Aalto
VTT Microelectronics
P.O. Box 1208 (Tietotie 3 Espoo)
FIN-02044 VTT
Finland
E-mail: timo.aalto@vtt.fi

Mikko Harjanne
Helsinki University of Technology
Optoelectronics Laboratory
P.O. Box 3500 (Tietotie 3 Espoo)
FIN-02015 Espoo
Finland

Markku Kapulainen
VTT Microelectronics
P.O. Box 1208 (Tietotie 3 Espoo)
FIN-02044 VTT
Finland

Abstract. A novel method has been developed for measuring the rotational angle of a fiber's or a waveguide's polarization axis with respect to a reference angle. The reference angle is the polarization axis of the measuring device. The method also gives the true polarization extinction ratio of the measured fiber or waveguide. The method is suitable for the characterization and rotational alignment of polarization-maintaining waveguides and fibers. In particular, the method can be used to rotationally align the fiber-waveguide interconnections during waveguide characterization. The measuring device is either a linear polarizer or a polarization splitter that is accurately rotated with respect to the device under test. According to the experiments with a polarization-maintaining fiber, the method is very easy and inexpensive to implement, and the angular accuracy can be better than 0.2 deg. [DOI: 10.1117/1.1600730]

Subject terms: optical waveguide; polarization-maintaining fiber; characterization; fiber-waveguide coupling; polarization; polarization axis; polarizer; polarization splitter.

Paper AWGE014 received Jan. 24, 2003; revised manuscript received Mar. 12, 2003; accepted for publication Mar. 24, 2003.

1 Introduction

Most of applications in optical telecommunication are based on using randomly polarized light, because the available polarization-maintaining fibers (PMFs) are clearly too expensive for long transmission links. The polarization-dependent loss (PDL) and the polarization mode dispersion (PMD) of devices are minimized to have sufficiently static operation during the polarization fluctuations that cannot be avoided in optical networks. The widely used single-mode fibers (SMFs) cannot maintain the polarization state of the light because of their negligible polarization extinction ratio (PXR). However, they have a weak birefringence that changes as a function of temperature, wavelength, and stress along the fiber. This induces time-dependent variations in both state of polarization and PMD of the fiber's output. Due to their statistical behavior, these fluctuations have a finite probability of becoming very strong.[1] When the data rates rise, the polarization problems become more difficult to handle. At very high data rates, active compensator devices can be used to eliminate the PMD caused by long fiber links.[2–4] They may also be used to stabilize the polarization to a fixed polarization state.[5]

Inside the network nodes, there are two possibilities for handling polarization problems. The devices can be made either sufficiently polarization independent or sufficiently polarization maintaining. In the former case, randomly polarized light may be used, while in the latter case, only well-defined polarization is used. In either case, it is essential to be able to accurately characterize the polarization properties of the devices.

The polarization characteristics of optical devices are often determined by using a polarization scrambler at the input, so that the maximum power variation at the output gives the PDL of the device. Reliable results require that the polarization scrambler scan the whole Poincaré sphere very densely. According to another method, the principal states of polarization (PSPs), or the polarization eigenmodes for continuous waves, are first determined from the device and input light is then coupled selectively to one PSP at a time.[4] The PDL can then be detemined as the ratio of two output powers, corresponding to the two different input polarizations. By comparing the power ratio of the two principal states of polarization at the output, one can also determine the polarization extinction ratio of the device for both input polarizations. This method is not very practical in the characterization of standard single-mode fibers and other such devices that do not have fixed principal states of polarization. However, in many other devices that have some kind of structural symmetry (see Fig. 1), the PSPs correspond to fixed linear polarization states that are identical at the input and output. This does not necessarily require a good PXR value. Such fixed principal states of polarization are referred to as the polarization modes or the polarization axes of the device, and they exist in all polarization-maintaining fibers and in many integrated optical components. In a PMF, the polarization modes lie along the so-called slow and fast axis, while in many integrated optical waveguides they lie horizontally [transverse-electric (TE) or quasi-TE mode] and vertically [transverse-magnetic (TM) or quasi-TM mode] with respect to the substrate.[3,5]

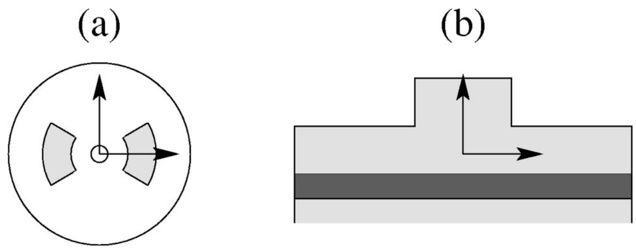

Fig. 1 Schematic cross sections of structures with fixed PSPs: (a) polarization-maintaining fiber and (b) integrated optical waveguide.

Table 1 Jones matrices of some ideal components (β_i = propagation constant, z = longitudinal coordinate, and α = rotational angle).

Fiber/waveguide	Rotational junction	Polarizer
$\begin{bmatrix} \exp(i\beta_1 z) & 0 \\ 0 & \exp(i\beta_2 z) \end{bmatrix}$	$\begin{bmatrix} \cos(\alpha) & \sin(\alpha) \\ -\sin(\alpha) & \cos(\alpha) \end{bmatrix}$	$\begin{bmatrix} \cos^2(\alpha) & \cos(\alpha)\sin(\alpha) \\ \cos(\alpha)\sin(\alpha) & \sin^2(\alpha) \end{bmatrix}$

When using polarization modes to characterize components, the input light must be carefully coupled to only one polarization mode at a time. As a PMF is typically used for input coupling, the rotational alignment between the device and the PMF input must be very accurate. Furthermore, when using different polarizing and polarization-maintaining components in any characterization, communication, or sensing systems, all the interconnections must be rotationally aligned with high precision to minimize the polarization cross talk between different polarization modes.

Several methods for the rotational alignment of a PMF have already been proposed.[6–9] They are typically based on changing the phase difference between the polarization modes continuously and by simultaneously rotating a polarizer in front of the PMF. The phase difference can be varied, e.g., by heating,[6,7] stretching, or pressing the fiber, or by tuning the wavelength.[8,9] Each of these methods requires a long piece of fiber, a long measurement time, simultaneous variation of several measurement parameters, or some complicated and expensive equipment, such as a polarization analyzer or a tunable laser. The accuracy of the methods typically varies between 0.2 and 1 deg. There are also other methods that rely on optical observation of the fiber end, but these typically have an accuracy of 1 deg or worse.

A novel method for accurate determination of rotational angles between different polarizing and polarization-maintaining components is described and demonstrated. The method is applicable to such fibers and waveguides that have fixed principal states of polarization and a finite polarization extinction ratio. When compared to earlier methods, the new method is particularly simple and inexpensive to implement.

2 Jones Matrix Theory

There are two alternative ways to analyze polarization by using matrix algebra, namely, the Stokes and Jones methods. Both of them define the states of polarization as vectors, and the polarization changes due to optical components as matrices. The Stokes vectors and the associated Müller matrices take into account both the polarized and depolarized light, while the Jones vectors and matrices can only handle polarized light. In this work, the Jones vectors and matrices are used for mathematical simplicity, but all the results can be converted into Stokes vectors and Müller matrices.[10,11]

When the Jones vectors and matrices are used, some basic assumptions and approximations are made. First, light is assumed to be fully polarized. Second, light is described only by two complex values that represent two transverse and orthogonal components of a harmonic plane wave. We assume that the PSPs of the optical components are linear polarization states, and the two complex values represent the two polarization eigenmodes, e.g., the slow and fast axis of a PMF [see Fig. 1(a)] or the TE and TM modes of a waveguide [see Fig. 1(b)]. These complex values can be represented as a Jones vector

$$\mathbf{J} = \begin{bmatrix} E_1 \exp(i\varphi_1) \\ E_2 \exp(i\varphi_2) \end{bmatrix} = E_1 \exp(i\varphi_1) \begin{bmatrix} 1 \\ \exp(i\Delta\varphi)/r \end{bmatrix}, \tag{1}$$

where $r = E_1/E_2$ is the ratio of the amplitudes E_1 and E_2, and $\Delta\varphi = \varphi_2 - \varphi_1$ is the phase difference between the two polarization components. The common factor in the latter expression can be dropped out if the absolute power and the absolute phase are not relevant.

Polarization transformation caused by an optical component or a rotational junction is described by a matrix equation

$$\mathbf{J}_{\text{out}} = \mathbf{M}\mathbf{J}_{\text{in}} = \begin{pmatrix} j_{11} & j_{12} \\ j_{21} & j_{22} \end{pmatrix} \begin{bmatrix} E_{1,\text{in}} \exp(i\varphi_{1,\text{in}}) \\ E_{2,\text{in}} \exp(i\varphi_{2,\text{in}}) \end{bmatrix} = \begin{bmatrix} E_{1,\text{out}} \exp(i\varphi_{1,\text{out}}) \\ E_{2,\text{out}} \exp(i\varphi_{2,\text{out}}) \end{bmatrix}, \tag{2}$$

where $\mathbf{M}$ is the Jones matrix and subscripts "in" and "out" refer to the situation before and after a component or a junction. The Jones vectors and matrices are associated with a certain coordinate system that is aligned with respect to the polarization axes of the fiber, waveguide, or another component. Therefore, rotation of the coordinate system between different components must be carried out by using an appropriate Jones matrix. In the following, such a rotational junction is simply referred to as a junction. The Jones matrices of some ideal components are listed in Table 1.

The true PXR of light that propagates along a fiber (or a waveguide) or that comes out of the fiber is defined to be the ratio of the two amplitudes (E_1, E_2) of the Jones vector squared, and is never less than one. In relative units, PXR $= r^2 (E_1 \geqslant E_2)$ or $1/r^2 (E_1 \leqslant E_2)$, and in decibel units is

$$\text{PXR} = |20 \log(E_1/E_2)| \text{dB} = |20 \log(r)| \text{dB}. \tag{3}$$

In real polarization-maintaining fibers (and waveguides), the maximum PXR is typically below 35 dB due to the finite polarization cross-talk inside the fibers. However, the main limiting factor for the PXR in optical systems is the

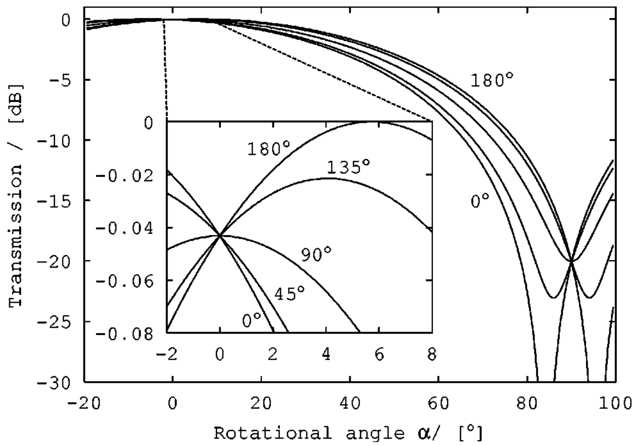

Fig. 2 Calculated transmission through an ideal polarizer when $PXR_{in} \equiv 20$ dB.

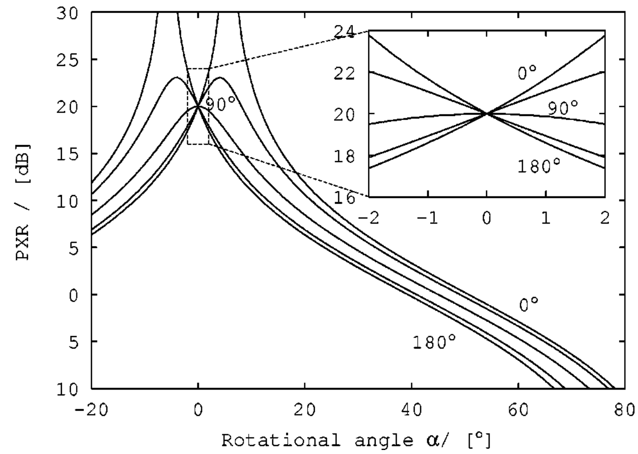

Fig. 3 Calculated PXR_{out} after a rotary joint (angle α) when $PXR_{in} \equiv 20$ dB. Each curve has a fixed phase difference (0, 45, 90, 135, or 180 deg).

polarization cross-talk caused by the rotationally misaligned junctions between the fibers (and waveguides). This can be seen by calculating the PXR change in a junction, where a polarization axis on one side of the junction has a rotational angle α with respect to a polarization axis on the other side of the junction. With a given amplitude ratio r, phase difference ($\Delta\varphi$), and angle (α), the Jones vector at the output (excluding the common factor) becomes

$$\mathbf{J}_{out} = \begin{bmatrix} \cos(\alpha) & \sin(\alpha) \\ -\sin(\alpha) & \cos(\alpha) \end{bmatrix} \begin{bmatrix} 1 \\ \exp(i\Delta\varphi)/r \end{bmatrix} = \begin{bmatrix} \cos(\alpha) + \sin(\alpha)\exp(i\Delta\varphi)/r \\ -\sin(\alpha) + \cos(\alpha)\exp(i\Delta\varphi)/r \end{bmatrix}. \quad (4)$$

The output PXR (PXR_{out}) can then be obtained as the ratio of the two output amplitudes squared. The amplitude of the first output polarization component is plotted in Fig. 2 as a normalized function of α with five different values of $\Delta\varphi$ and a fixed input PXR ($PXR_{in} \equiv 20$ dB). The result is identical with the transmission through a polarizer with an angle α. The second polarization component corresponds to a ± 90 deg rotation with respect to the first component. It can be seen from Fig. 2 that the smaller polarization component ($\alpha \approx 90$ deg) varies much more strongly with respect to α and $\Delta\varphi$ than the larger component ($\alpha \approx 0$ deg). Therefore, the smaller component dominates the dependence of PXR_{out} on α and $\Delta\varphi$ with a high PXR_{in}. With some simple algebra, the output PXR becomes

$$PXR_{out} = \left| 10 \log \left[\frac{r^2 + 2r\tan(\alpha)\cos(\Delta\varphi) + \tan^2(\alpha)}{r^2\tan^2(\alpha) - 2r\tan(\alpha)\cos(\Delta\varphi) + 1} \right] \right| \text{dB}. \quad (5)$$

In Fig. 3 the output PXR according to this formula has been plotted for a fixed input PXR ($PXR_{in} = 20$ dB) as a set of curves, so that each curve represents PXR_{out} as a function of α for a given $\Delta\varphi$. It should be noted that the plotted set of curves (not the individual curves) is symmetric and antisymmetric with respect to angles $\alpha = 0$ deg and $\alpha = 45$ deg, respectively. The set of curves has common crossing points wherever $\alpha = \pm N \cdot 90$ deg ($N = 0, 1, 2, 3$), i.e., when any two polarization axes are parallel. At the crossing points, $PXR_{out} = PXR_{in}$. It can also be seen that close to the crossing points PXR_{out} varies particularly rapidly with respect to both α and $\Delta\varphi$, and the maxima of the curves do not associate with any constant angle. With appropriate α and $\Delta\varphi$, the output PXR can be significantly higher than the input PXR. For example, with $\Delta\varphi = \pm N \cdot 180$ deg, $\alpha = \pm a\tan(1/r)$, and $r > 1$, PXR_{out} can reach infinity, corresponding to a linear polarization state. However, with appropriate $\Delta\varphi$, the output PXR may also decrease very rapidly as a function of α.

Successive junctions increase the fluctuation of the PXR_{out}, as can be seen from Fig. 4. In general, the average PXR_{out} degrades and the range of the variation increases as the number of junctions and the magnitude of the angles increase. The results in Fig. 4 are based on the assumption

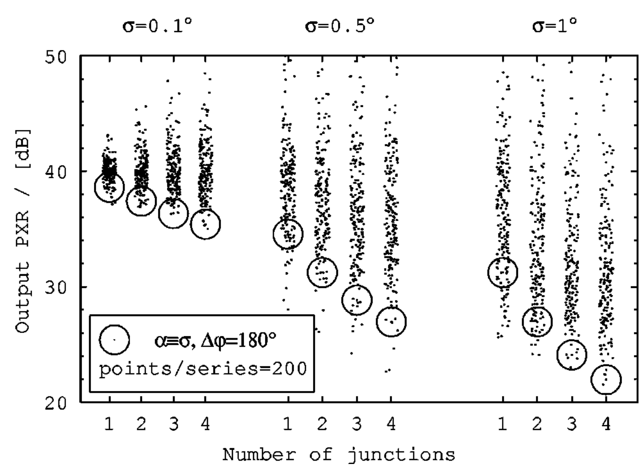

Fig. 4 Statistical analysis of PXR fluctuation after successive junctions. The misalignment (α) in each junction was varied randomly by assuming a normalized distribution and a given standard deviation (σ), while the phase difference ($\Delta\varphi$) was varied randomly in the range 0 to 360 deg. $PXR_{in} = 40$ dB before the first junction, and the number (N) of successive junctions varies from 1 to 4. Circles correspond to $\alpha \equiv \sigma$ and $\Delta\varphi \equiv 180$ deg.

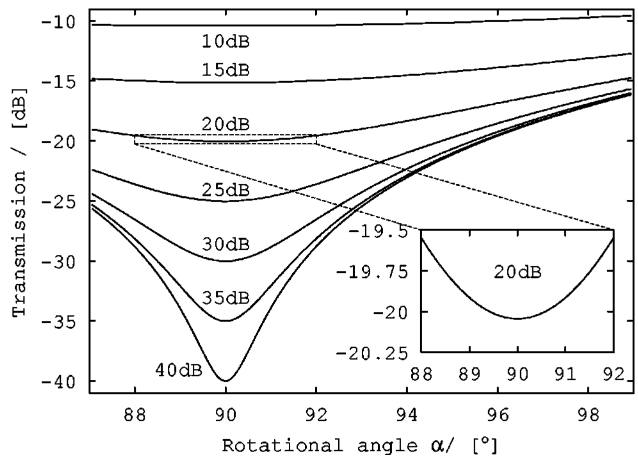

Fig. 5 Calculated transmission of broadband light through an ideal polarizer when the true PXR_{in} varies between 10 and 40 dB.

that both $\Delta\varphi$ and α vary randomly (α according to a normal distribution). The results clarify the need to minimize the misalignments in the junctions when a static and high PXR_{out} is needed.

When the rotational angle of a fiber's polarization axis is measured or optimized, it must first be defined with respect to some physical reference angle of a measuring device, e.g., the transmission or blocking direction of a linear polarizer. Therefore, this reference angle corresponds to the origin of the α scale and to one crossing point of the theoretical set of curves (see Figs. 2 and 3). In the beginning of a measurement, the angle α is unknown and a separate measurement scale (β) must be used to control the possible rotation of a measuring device with respect to the fiber. It is here defined that the origin of the α scale and the associated crossing point of the theoretical set of curves correspond to a certain crossing point angle β_{CP} on the measurement scale (β). If β_{CP} can be determined, then also the fiber's angle $\alpha=\beta-\beta_{CP}$ can be obtained and set to any desired value.

Another definition for the PXR is based on detecting the minimum and maximum transmission (P_{min},P_{max}) of a light beam through a rotated polarizer. This so called free-space PXR (PXR_{FS}) is defined as

$$PXR_{FS}=10\log(P_{max}/P_{min})\text{dB}. \quad (6)$$

As is evident from Figs. 2 and 3, this method cannot be used directly to give reliable results for the PXR or the rotational angle of a fiber, unless the effect of $\Delta\varphi$ is somehow eliminated. However, when a sufficiently broadband light source is used, $\Delta\varphi$ averages out of Eq. (5) and the results correspond to a case where $\Delta\varphi\equiv 90$ deg. This validates the use of Eq. (6) for characterizing a fiber output only when $\Delta\varphi$ averages out of the results. Theoretical curves for broadband transmission through a polarizer with different input PXRs are shown in Fig. 5.

3 Novel Method for Rotational Alignment

Due to the additional dependence of PXR_{out} on $\Delta\varphi$, the determination of PXR and the rotational angle α of a fiber is not experimentally trivial. The simple rotation of a polarizer in front of the fiber can give misleading results if $\Delta\varphi$ is unknown (see Fig. 2). Continuous rotation of a polarizer and a simultaneous scanning of $\Delta\varphi$ can point out an angle ($\alpha\approx N\cdot 90$ deg), where the dependence of PXR_{FS} on $\Delta\varphi$ is at a minimum or the minimum of $PXR_{FS}=f(\Delta\varphi)$ has a maximum. However, the continuous scanning of both α and $\Delta\varphi$ makes the measurement relatively slow, and the accuracy of the method is difficult to estimate. The whole definition of PXR for a fiber (or waveguide) is meaningful only if the PSPs are fixed, but the finding of a minimum or a maximum signal does not guarantee this.

As is shown next, Eq. (5) and the corresponding set of curves (Fig. 3) can be used to easily determine both α and PXR of a fiber (or waveguide). The basic principle of this method is that first, two or more curves, similar to those in Figs. 2 and 3, are measured by varying the measurement angle β in the junction between the fiber and the measuring device. Then the crossing point of the measured curves is determined. This point directly corresponds to β_{CP} and the PXR value of the fiber (PXR_{in}, before the junction). Transitions between different curves are done by somehow changing the phase difference $\Delta\varphi$ of the fiber's output. One advantage of the new method is that one does not need to know $\Delta\varphi$ or to continuously vary it. It is sufficient to induce such changes in $\Delta\varphi$ that at least two measured curves are clearly different. These changes can be realized either by modifying the light guiding properties of the fiber or by tuning the wavelength. The former can be easily done by heating, stretching, or pressing the fiber.

Transmission curves (Fig. 2) can be measured by rotating a polarizer in front of the fiber end. PXR_{out} curves can be obtained by calculating the ratio of transmissions in perpendicular angles (β, $\beta\pm 90$ deg). Alternatively, the PXR_{out} curves can be directly measured by calculating the ratio of two output powers that originate from a rotatable polarization splitter.

The measured curves are not identical with the theoretical curves because of the finite accuracy in optical power and angle (β) measurements, the instabilities of the fiber and the measurement system, the depolarized fraction of light, the finite bandwidth of the light, and the wavelength fluctuations. Therefore, the position of the crossing point may not be explicitly determined. There are several possibilities for postprocessing the results. One may fit the theoretical set of curves to the results, or one may also fit each curve individually by just assuming a fixed crossing point angle β_{CP} and taking into account the possible PXR fluctuations. Also, the measured points can all be connected with interpolated curves. This typically produces several crossing points, and β_{CP} can then be obtained by appropriately averaging them. The measurement error in both α and PXR can be estimated based on the quality of fitting or the variation between the different crossing points. In both cases, the measurement accuracy for β_{CP} can be clearly better than the angular spacing between individual measurement points, unlike in many alternative methods.

4 Results

The functionality of the new method was demonstrated by measuring the angle of a polarization-maintaining fiber's polarization axis with respect to the blocking direction of a

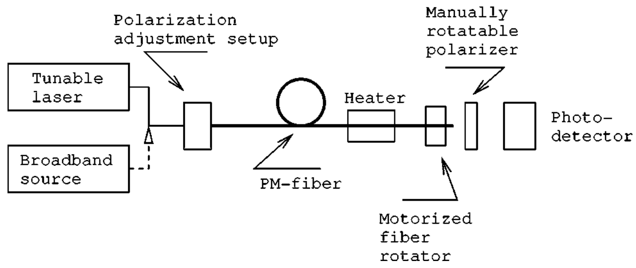

Fig. 6 Schematic layout of the measurement setup.

thin film near-infrared polarizer. The extinction ratio of the polarizer is better than 40 dB around the 1550-nm wavelength. The measured fiber is used as an incoupling fiber in a waveguide characterization setup, so a succesful fiber alignment can be readily exploited in waveguide measurements. Due to the flatness of the waveguide chips, they can be easily aligned with respect to the calibrated angle of the polarizer.

The experimental setup for measuring the fiber is shown in Fig. 6. Light is launched either from a narrowband laser ($\lambda = 1550$ nm) or a broadband LED into a 7-m-long polarization-maintaining fiber (PANDA) via a polarization-adjustment setup. The polarization and power of the light that couples into the fiber can be controlled and stabilized. The light, originating from the bare output end of the fiber, is guided through the manually rotatable polarizer to a photodetector. The line grid of the measurement scale was as high as 2 deg and, therefore, the relative accuracy of the first angle readings was only 0.5 deg. However, to obtain more accurate results, a motorized fiber rotator was constructed to turn the fiber with respect to the polarizer. This improved the accuracy in the last measurements down to 0.05 deg. Before starting the actual measurements, the polarization axes at the output of the fiber were determined coarsely by rotating the polarizer (or the fiber) and maximizing PXR_{FS} with the laser source. Then the accurate angle was determined by measuring sets of curves and locating the crossing points. The phase was varied either by changing the wavelength, by simply moving the fiber on a table, or by heating an approximately 8-cm-long piece of the fiber.

When using wavelength tuning, it was found that only a 1-nm wavelength step is sufficient to cause a 2π phase difference. The required wavelength change is so small that the wavelength dependences of the polarizer and the polarization-adjustment setup do not affect the results. Figure 7 shows both the measured PXR_{out} values and the theoretical curves that are based on Eq. (5) and fitted to the results. The fiber's PXR (PXR_{in}) and the crossing-point angle β_{CP} were used as common fitting paremeters, while $\Delta\varphi$ was fitted separately for each curve. As can be seen from Fig. 7, the theoretical curves and measurement results agree very well. The accuracy of the results is limited by the coarse measurement scale of the manually rotated polarizer. The final accuracy of β_{CP} is slightly better than the 0.5 deg accuracy of the individual angle readings, because an appropriate curve fitting can partially average out the angle reading errors. This was verified by monitoring the fitting quality, while β_{CP} was slightly varied around its optimally fitted value. Detuning β_{CP} by ± 0.5 deg evidently degraded the fitting quality. The accuracy was also successfully confirmed by connecting the measured points with straight lines and by checking that the angular variation between different crossing points was below 0.5 deg.

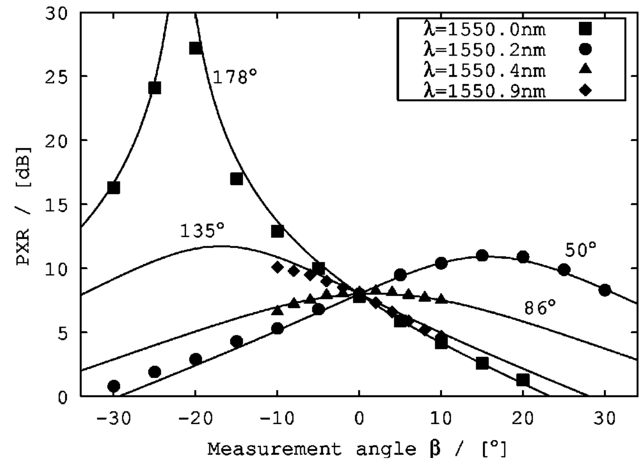

Fig. 7 Measurement results and fitted theoretical curves obtained by wavelength tuning.

The phase difference $\Delta\varphi$ was also tuned by simply moving the fiber on a table. Changing the direction or the amount of the loose fiber loops was sufficient to induce significant phase changes. Movements are also expected to cause slight variation in the PXR value. The phase change does not stabilize immediately after the movements, because the fiber loops experience microscopic movements after repositioning. Therefore, the measured curves, shown in Fig. 8, do not correspond to fully stabilized phase differences and a common PXR. The measurement accuracy is again better than 0.5 deg, and is mainly limited by the accuracy of the rotational scale. This was verified with the same principles as in the case of wavelength tuning.

Heating and motorized rotation of the fiber was found to be the most accurate measurement method. Figure 9 shows PXR_{out} as a function of β with different temperatures when the motorized fiber rotator was used. Only a couple of degrees temperature change is enough to change $\Delta\varphi$ signifi-

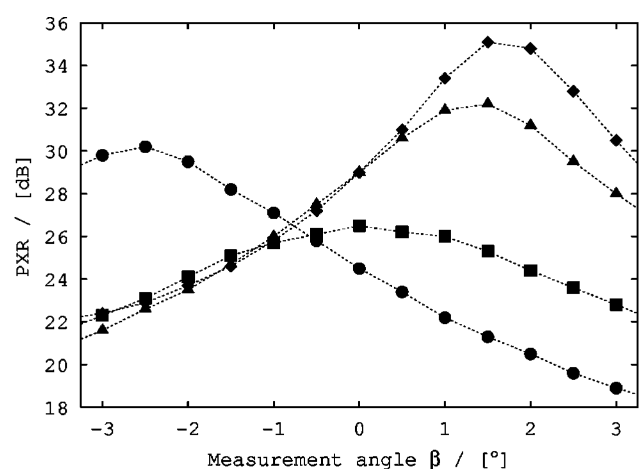

Fig. 8 Measurement results obtained by moving the fiber.

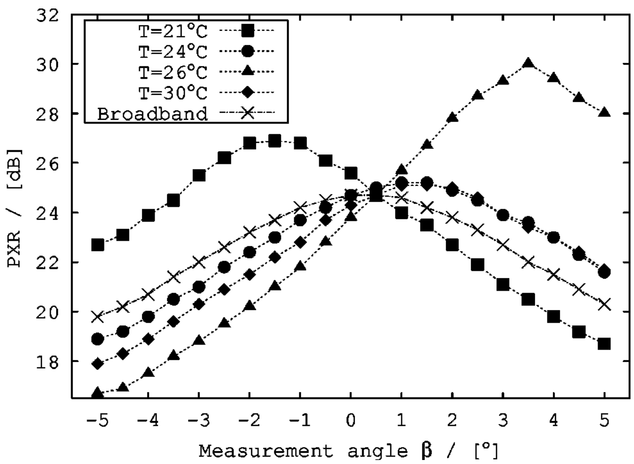

Fig. 9 Measurement results obtained by heating the fiber (filled symbols) and by using a broadband light source (thin crosses). Coarse angle variation.

cantly. Based on the results, the fiber angle was corrected toward the origin of the β scale, and a second set of curves was measured with a finer angular grid. This set of curves is shown in Fig. 10. In both cases, the measurements were carried out at four different temperatures. Based on Fig. 10 and the same criteria as with the previous phase tuning methods, the accuracy of β_{CP} is estimated to be better than 0.2 deg. For comparison, the measurement of each set of curves (Figs. 9 and 10) was followed by a PXR_{FS} measurement. In this procedure, a PXR_{out} curve was measured by using the broadband light source. These results agree well with the new method.

5 Conclusions

The best way to maintain a stable and sufficiently high PXR in a polarization-maintaining optical system is to use highly linear input polarization and very accurately aligned rotational junctions. The required rotational accuracy depends on the number of junctions, the polarization crosstalk induced by the components themselves, the required minimum PXR, and the tolerable PXR fluctuation. For most applications, the accuracy should be better than 0.5 deg, but for some applications the improvement of accuracy down to 0.1 deg is justified.

A novel method for the rotational alignment of polarization-maintaining fibers is presented and demonstrated. The best results are obtained by heating the fiber and by using a motorized fiber rotator. The measurement accuracy is better than 0.2 deg. Also, λ tuning and mechanical movement of the fiber are used to change the phase difference, but these methods were somewhat less accurate (0.5 deg). This is mostly due to the poor rotation accuracy (0.5 deg) of the manually rotated polarizer used in these measurements. By using curve fitting, the final results can be slightly better than the rotation accuracy.

The new method can be readily used in waveguide characterization, where the PMF must be carefully aligned with an integrated optical waveguide. It should also be possible to apply the method to the direct measurement of a waveguide's rotational angle. However, this would require a motorized rotation of the polarizer, because the manual polarizer rotation is less accurate than the straightforward alignment by using a rotationally calibrated flat plate under the chip. For short waveguides, a large amount of wavelength tuning is necessary, and this requires a stable input PXR with respect to λ. When heating a waveguide chip, the

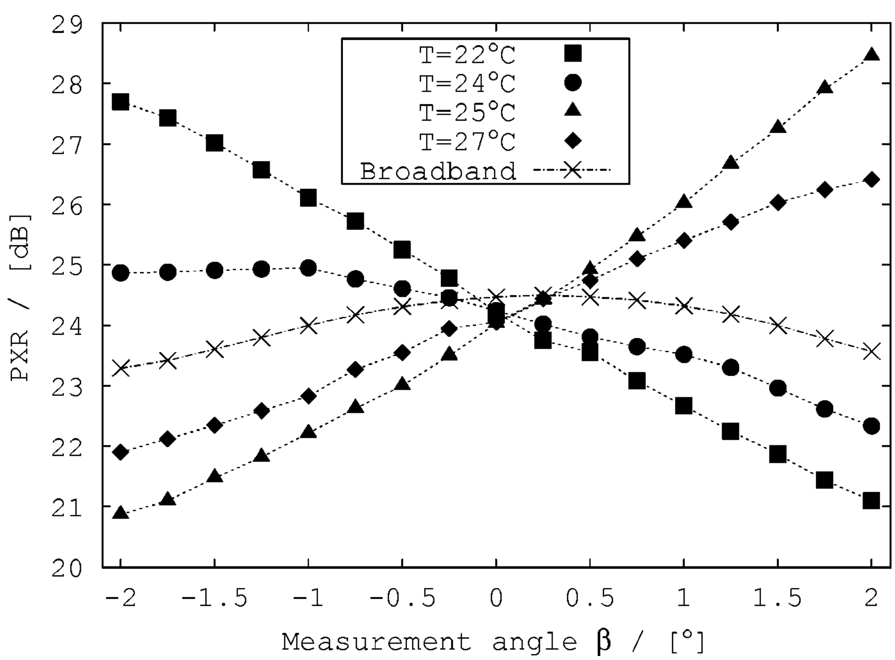

Fig. 10 Measurement results obtained by heating the fiber (filled symbols) and by using a broadband light source (thin crosses). Fine angle variation after angle adjustment.

stability of the input coupling also requires special attention.

Acknowledgments

The authors thank Markku Rönö for his assistance in the work and Jouni Nygård for building the motorized fiber rotator.

References

1. D. Wang and C. R. Menyuk, ''Calculation of penalties due to polarization effects in a long-haul WDM system using a Stokes parameter model,'' *J. Lightwave Technol.* **19**(4), 487–494 (2001).
2. N. Kikichi, ''Analysis of signal degree of polarization degradation used as control signal for optical polarization mode dispersion compensation,'' *J. Lightwave Technol.* **19**(4), 480–486 (2001).
3. F. Heismann, ''Integrated-optic polarization transformer for reset-free endless polarization control,'' *IEEE J. Quantum Electron.* **25**(8), 1898–1906 (1989).
4. H. Sunnerud, C. Xie, M. Karlsson, R. Samuelson, and P. A. Andrekson, ''A comparison between different PMD compensation techniques,'' *J. Lightwave Technol.* **20**(3), 368–378 (2001).
5. W.-Y. Hwang, M.-C. Oh, H. Park, J.-H. Ahn, S. G. Han, and H.-G. Kim, ''Polarization stabilizer using a polarization splitter and a thermooptic polymer waveguide device,'' *IEEE Photonics Technol. Lett.* **10**(12), 1736–1738 (1998).
6. N. Caponio and C. Svelto, ''A simple angular alignment technique for a polarization-maintaining-fibre,'' *IEEE Photonics Technol. Lett.* **6**(6), 728–729 (1994).
7. G. R. Walker and N. G. Walker, ''Alignment of polarization-maintaining fibres by temperature modulation,'' *Electron. Lett.* **23**(13), 689–691 (1987).
8. A. Ebberg and R. Noe, ''Novel high precision alignment technique for polarization maintaining fibres using a frequency modulated tunable laser,'' *Electron. Lett.* **26**(24), 2009–2010 (1990).
9. Y. Ida, K. Hayashi, M. Jinno, T. Horii, and K. Arai, ''New method for polarization alignment of birefringent fibre with laser diode,'' *Electron. Lett.* **21**(1), 18–21 (1985).
10. S.-M. F. Nee, ''Depolarization and principal Müller matrix measured by null ellipsometry,'' *Appl. Opt.* **40**(28), 4933–4939 (2001).
11. D. S. Kliger, J. W. Lewis, and C. E. Randall, *Polarized Light in Optics and Spectroscopy*, Academic Press, Inc., New York (1997).

Timo Aalto received his MSc degree in physics from the Helsinki University of Technology (HUT) in 1998. His major was optoelectronics and he is now doing his PhD studies around the same subject. He has worked at the VTT Center for Microelectronics since 1997. His research interests are the design, simulation, fabrication, and characterization of silicon-based waveguides, and especially silicon-on-insulator waveguides.

Mikko Harjanne received his MSc degree from Helsinki University of Technology (HUT) in 2003, his major being optoelectronics. Since his graduation he has worked at the Optoelectronics Laboratory at HUT.

Markku Kapulainen received his MSc degree in physics from the Helsinki University of Technology (HUT) in 2001. He has worked at the VTT Center for Microelectronics since 2001.